Color uniformity in spotlights optimized with reflectors and TIR lenses

Anne Teupner, Krister Bergenek, Ralph Wirth, Pablo Benítez, and Juan Carlos Miñano

Abstract: We analyze the color uniformity in the far field of spotlight systems to estimate visual perception with a merit function derived from human factor experiments. A multi-colored light-emitting diode (LED) light engine with different light mixing levels is combined with several reflectors and total internal reflection (TIR) lenses. The optimized systems are analyzed at several color uniformity levels with regard to the efficiency, peak luminous intensity and dimensions. It is shown that these properties cannot all be optimized at the same time. Furthermore, excellent color uniformity can be reached by a light mixing layer in the light engine or by adding mixing elements to the secondary optics.

1. Y. Ohno, "Spectral design considerations for white led color rendering," Opt. Eng. **44**(11), 111302 (2005).
2. I. Moreno and U. Contreras, "Color distribution from multicolor LED arrays," Opt. Express **15**(6), 3607–3618 (2007).
3. F. R. Fournier, "A review of beam shaping strategies for LED lighting," Proc. SPIE **8170**, 817007 (2011).
4. C.-C. Sun, I. Moreno, Y.-C. Lo, B.-C. Chiu, and W.-T. Chien, "Collimating lamp with well color mixing of red/green/blue LEDs," Opt. Express **20**(1 S1), A75–A84 (2012).
5. E. Chen, R. Wu, and T. Guo, "Design a freefrom microlens array module for any arbitrary-shape collimated beam shaping and color mixing," Opt. Commun. **321**, 78–85 (2014).
6. A. Teupner, K. Bergenek, R. Wirth, J. C. Miñano, and P. Benítez, "Optimization of a merit function for the visual perception of color uniformity in spot lights," Color Res. Appl. (2014), doi:10.1002/col.21888.
7. G. M. Johnson, X. Song, E. D. Montag, and M. D. Fairchild, "Derivation of a color space for image color difference measurement," Color Res. Appl. **35**(6), 387–400 (2010).
8. X. Zhang and B. A. Wandell, "A spatial extension of cielab for digital color-image reproduction," J. Soc. Inf. Disp. **5**(1), 61–63 (1997).
9. A. Teupner, K. Bergenek, R. Wirth, J. C. Miñano, and P. Benítez, "Optimization of optical systems for LED spot lights concerning the color uniformity," Proc. SPIE **9190**, 91900J (2014).
10. J. Chaves, A. Cvetkovic, R. Mohedano, O. Dross, M. Hernandez, P. Benitez, J. C. Miñano, and J. Vilaplana, "Inhomogeneous source unifomization using a shell mixer Koehler integrator," Proc. SPIE **8550**, 85502X (2012).

1. Introduction

The design of spotlights involves the combination of a light source with a secondary optical element to collimate light in the far field into a spot. Multi-colored light-emitting diode (LED, phosphor-converted green plus monochromatic red and blue source, also called hybrid LEDs) light sources are required for obtaining high quality lighting with tunable white light spectrum. Such sources provide a high color rendering index (CRI), more vivid colors and higher efficacy in contrast to sources based on phosphor blended solutions [1]. The combination of spatially or angularly separated color in the light engine and optical elements determines the appearance of colors and patterns in the far field [2]. In this study, we attempt to optimize the full width half maximum (FWHM) angle and efficiency of spotlighting systems with reflectors and TIR lenses [3]. The performance of these spotlights is compared for given qualities of color uniformity with regard to efficiency and peak luminous intensity.

2. Color uniformity U_{sl} in spotlights

In order to achieve this objective, it is necessary to adopt an evaluation method that analyzes the color uniformity of the far field based on visual perception. In general, color uniformity evaluation in spatially defined far fields is based on differences with respect to mean color values [4, 5].

Various combinations of LED light engines and optical elements produce a wide range of color appearances in spotlights [Fig. 1]. In essence, red, green and blue colors from RGB-LEDs or blue-yellow light from converted light engines appear. These lead to the formation of patterns such as rings (multiple, segmented or fragmented), dots and imaged LEDs in the far field when the spotlights are projected onto a wall.

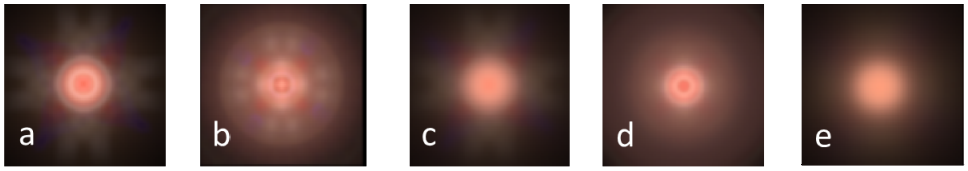

Fig. 1. Simulated far fields of five different spotlights, (a - d) are TIR lens spotlights, and (e) is a reflector spotlight, all with multi-colored light engines.

The far field illumination was analyzed. For visualization, the images of all simulated spotlights are shown with regard to a warm white reference spotlight of 2700 K.

An evaluation method related to visual color perception has previously been proposed [6] for the analysis of color uniformities. In human factor experiments, several spotlight far fields had to be evaluated by observers. The perceived order of the tested far fields was correlated with mathematical descriptions of spatial color distributions. The merit function U_{sl} [Eq. (1)] is based on a linear regression of four separate functions resulting from best found correlation with the perceived order of the visually evaluated spotlights. A weighting performed with the contrast sensitivity function [7] ensures an evaluation that is dependent on distance and visual sensitivity. Furthermore, a luminance cut-off is implemented; it was set to 10% of the maximum luminance in the far field of the spotlight. The merit function is expressed as:

$$U_{sl} = a_1 \cdot \Delta ab_{mean} + a_2 \cdot Grad_{ab} + a_3 \cdot S_{rad} + a_4 \cdot S_{lin} \qquad (1)$$

This equation is presented in the CIELAB color space [8], with color values a^* and b^*. The function Δab_{mean} expresses the mean of the color difference between each pixel and the weighted average color of the considered far field. The function $Grad_{ab}$ calculates the difference of color between neighboring pixels. The parameters S_{rad} and S_{lin} describe the smoothness of the radial and linear color gradients, respectively. They were used to detect the maximum standard color deviation on the radial and angular axes. The coefficients a_1, a_2, a_3 and a_4 are optimized to ensure a very strong correlation between U_{sl} and the perceived order. The optimization of the coefficients leads to a Spearman correlation coefficient of *0.93* for a_1, a_2, a_3, and a_4 values of 2.5, 8, 3 and 1, respectively [9].

The U_{sl} scale was classified into levels ranging from excellent to insufficient color uniformity [Fig. 2]. The classification was derived from an additional human factor experiment wherein subjects had to grade separately presented spotlights. Spotlights reaching U_{sl} values lower than 30 have perfectly mixed color uniformity and the human eye cannot detect color inhomogeneities. The minimum U_{sl} value was limited due to measuring noise, number of simulation rays, and resulted color accuracies.

The comparison of measurement and simulation results for U_{sl} of four spotlights showed aberrations of U_{sl} not larger than 10% assuming adequate simulation parameters [9]. The evaluation of far fields is not limited to multi-colored LEDs but also for phosphor converted light engines or RGB LEDs.

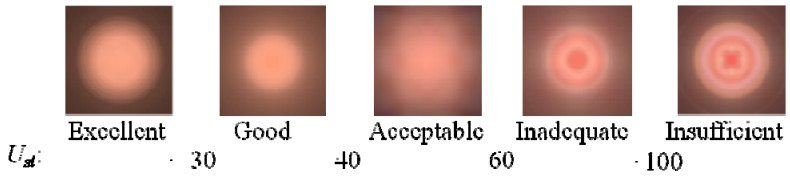

Fig. 2. Levels of perceived color uniformity in simulated spotlights with their corresponding far fields resulting of a LED light source in combination with different reflectors.

3. Optical system design

Several spotlighting systems comprising three different LED light engines and secondary optics (reflectors and TIR lenses) were optimized to a full width half maximum angle (FWHM) of 20° ± 1° and to high efficiency. On the one hand, color blending can be realized in light engine with scattering layers and particles of different densities. On the other hand, color mixing can be assigned to the secondary optics of the system. A combination of both mechanisms is also conceivable.

3.1 Light source

For the simulations, we created three multi-colored LED light engines (LE) [Fig. 3, background]. All three engines comprise the same setup and consist of 12 green converted chips, 5 red chips and 4 blue chips in a 9 mm diameter light-emitting area.

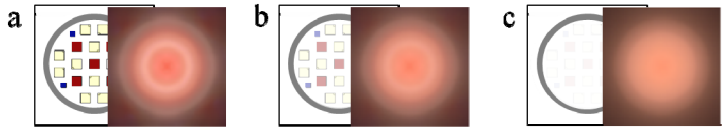

Fig. 3. The three setups of the light engine with a 9 mm diameter light-emitting area: background: (a) with clear cast, (b) low scattering particle density, (c) high scattering particle density; foreground: far fields of spotlights for each corresponding light engine and specular standard reflector. U_{sl} values are 145, 46 and 38 for (a), (b), and (c), respectively.

The light-emitting area is covered with a silicone volume cast for better light extraction from the chips. Scattering particles can be incorporated in this layer in order to improve color blending [Fig. 3, foreground]. Increasing the scattering particle density improves the color uniformity up to a certain level. However, the presence of a very high number of particles significantly decreases the mean free path of the light rays, and the local scattering effects increase. Consequently, a reduced amount of light is extracted, and no additional light mixing can be achieved. However, increasing the scattering particle concentration leads to lower extraction efficiencies due to losses in the scattering process [Fig. 4] and absorption of back-scattered light in the LED chips or on the substrate.

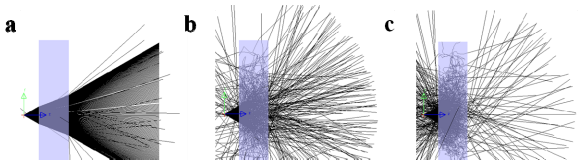

Fig. 4. Scattering process: a) no scattering particles are present and light passes through the layer without distortions; b) some scattering particles mix the rays and result in improved color blending and enlarge the FWHM angle; c) a very large number of scattering particles decrease the efficiency (reduced number of less forward traveling rays) and local scattering is too large to yield further improvements in color blending.

The light extraction from LE1 without scattering particles was normalized to 100%, and that from LE2 and LE3 features 99.5% and 94.9%, respectively.

3.2 Secondary optics

Several TIR lenses [Fig. 5(a)] and reflectors [Fig. 5(b)] were used for the study. Plain secondary optics and optics with facets or scattering surfaces are available. To one reflector [Fig. 5(b3)] we added an optical element called the shell mixer [10] which is an LPI patented dome element with a double sided Köhler lens array designed as an add-on to provide color blending of existing luminaries.

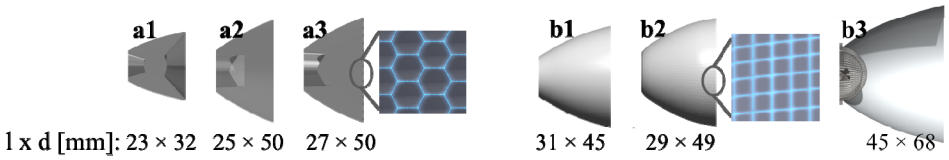

Fig. 5. Optimized optics: (a1) plain TIR lens, (a2) TIR lens with rough outer surface, (a3) TIR lens with lens array (18 × 18), (b1) plain reflector, (b2) reflector with 100 radial and 50 axial facets, (b3) plain reflector and shell mixer. The specifications in the second row represent the product of the dimension of each element length (l) and its diameter (d) [mm].

The diameter of the secondary optics was limited to 50 mm, which from an etendue conservation perspective easily enables a collimation to the targeted 20° FWHM angle for the 9 mm light source. Two secondary optics differed in dimensions. Spotlight a1 was smaller due to its biconvex central shape which supported the collimation into FWHM angle. Spotlight b3 is larger due to the application of the shell mixer (diameter of 27 mm) because the reflector had to fit around.

The systems were first optimized with LE2 and afterward applied to the other two engines. The TIR lenses were made of PMMA with a refractive index of 1.494. The reflectivity of the reflectors was assumed to be 90%. All the elements were simulated with perfect surface quality and geometry. A receiver at a distance of 2 m from the optical system was installed to record the far field and to detect data for the analysis.

4. Results

First, we compare the merit function U_{sl} for color uniformity for all combinations [Table 1]. There is a wide range for color uniformity levels in the system from excellent to insufficient color mixing.

Table 1. Overview of U_{sl} values for the optical systems: formed by the combination of the three light engines shown in Fig. 3 and the secondary optics in Fig. 4; table entries with the green background denote excellent color uniformity levels while yellow and red background entries denote acceptable and insufficient color uniformities, respectively.

	TIR lenses			Reflectors		
	a1	a2	a3	b1	b2	b3
LE1	179	117	29	145	87	21
LE2	109	76	26	46	57	22
LE3	40	31	20	38	29	13

Starting with the analysis of the light engines, there is a clear improvement of the color mixing level with better premixed light from the source. The better the mixing in the light engine is, the better is the far field appearance. The color mixing in the light engine is the basis for obtaining a uniform far field. There are two samples that already show excellent color mixing in combination with the unmixed LE1. The TIR lens with a lens array and the plain reflector with the shell mixer lead to excellent color uniformity levels independent of the light engine. Moreover, additional light mixing elements are useful in this regard and most of these elements clearly improve the color mixing level when combined with unmixed light engines like LE1. Excellent color uniformity is achieved either by adjusting the additional

mixing elements or by the use of mixed light engine LE3. Furthermore, always excellent color uniformity in the far field is achieved with the shell mixer. In general, the reflectors perform better than the TIR lenses with regard to U_{sl}.

The color uniformity is not arbitrarily adjustable, and it is limited to a minimum value for each spotlight as a combination of light engine and secondary optics. Using a specific light engine in combination with a secondary optics, U_{sl} is limited and not always perfect color uniformity could be reached by implementation of scattering layer in the light engine or mixing elements in the secondary optics.

However, excellent spotlights often exhibit lower efficiency. The best solution (b3, reflector with shell mixer) regarding color uniformity exhibits the poorest performance in terms of efficiency [Table 2] and peak luminous intensity [Table 3] due to the presence of the additional optical element. Light reflected back by Fresnel reflection is only partially recycled in the LE (up to 80%). The shell mixer was not optimized itself, its dimension was adjusted to the diameter of the light engine. Thus, a larger reflector was needed to reach the FWHM angle. The efficiency in relation to reflector b1 is lower. The efficiency with the same reflector but without shell mixer would be 4% to 6% higher, but with much worse color uniformity.

The efficiency of the optical systems depends mainly on reflection / refraction properties and the number of elements. In addition, for optical systems with the same secondary optics, the efficiency depends only on the light engine. This efficiency is reduced by about 5% from LE1 to LE3 for all systems. There is no significant difference in efficiency between reflectors and TIR lenses. The different efficiencies between the two reflectors are caused by the different optical shapes; the presence of facets does not decrease the efficiency.

Table 2. Efficiencies of the optical systems, measured at a spherical far field receiver around the optical system assuming that the system is encased. Light emitted from the optical front surface is represented as a percentage of the best system LE1-b1. Green-, yellow-, and red-background entries represent excellent, acceptable, and insufficient color uniformity levels, respectively.

	a1	a2	a3	b1	b2	b3
LE1	99.4	97.3	97.6	100.0	98.5	91.9
LE2	99.2	97.1	97.3	99.7	98.2	91.7
LE3	94.2	92.6	92.7	94.8	94.0	85.6

Table 3. Peak luminous intensity for all optimized systems as a percentage of the best system LE2-a1. Green-, yellow-, and red-background entries represent excellent, acceptable, and insufficient color uniformity levels, respectively.

	a1	a2	a3	b1	b2	b3
LE 1	96.9	85.3	80.5	73.7	59.8	58.2
LE 2	100	86.9	80.5	75.2	60.2	58.5
LE 3	96.6	83.9	77.0	73.4	57.4	56.6

In contrast to the efficiency, the differences in the peak luminous intensity are higher. These differences also result from unequal intensity distributions because the systems were optimized to FWHM and efficiency. Thus, the luminous intensity distribution differs [Fig. 6] for different spotlights. There are clear differences in the intensity distribution between TIR lenses and reflectors. Reflectors do not provide such high peak luminous intensities due to their shape and non parabolic profiles. The intensity is reduced through the introduction of additional mixing elements because the shape of the intensity distribution was changed. More light is spread outside the target area of the spotlight [Fig. 6, right].

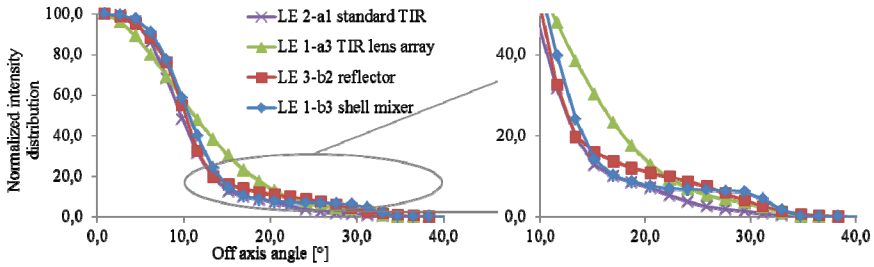

Fig. 6. Plot of luminous intensity distributions (normalized at 0°) for the four selected optical systems; left: complete intensity distribution, right: detailed intensity distribution of the edge of the spotlight far fields.

5. Discussion

Our results indicate that there is no single system with an overall excellent performance. However, there are systems that exhibit very satisfactory performances with regard to single categories. Excellent color mixing is provided by the shell mixer. The efficiency and peak intensity values are poor. For high efficiency, a plain reflector with a well-mixed light engine or a TIR lens array with an unmixed light engine is recommended. For high peak intensity, a standard TIR lens with a mixed engine is practicable but leads to poor color blending.

The difference between the light mixing in the engine and the optics is marginal. It is possible to generate light mixing in both parts with similar efficiency losses. A uniform far field is thus possible by using a well-mixed light engine (with any secondary optics) or secondary optics with mixing elements. Light mixing in the light engine is limited depending on the type of source, scattering layers, and LED configuration. In the present paper, perfect color uniformity could not be achieved only by scattering layers in the engine.

Color mixing with additional elements such as facets or rough surfaces is possible with accurately adjusted parameters (such as dimension, shape, and number of facets). Otherwise these elements only reduce the efficiency or peak luminous intensity without providing any color uniformity improvement. Furthermore, higher levels of collimation tend to downgrade the color uniformity.

Other properties for spotlights that need to be considered include near field properties and uniformity, sensitivity to colored shadows, variable luminance distribution, manufacturability, geometrical tolerances, and boundaries.

6. Summary

The evaluation of the color mixing level in the far field of spotlights by the merit function U_{sl} was realized by several optical systems. They were optimized with respect to a FWHM angle of 20° and compared at a similar color uniformity level referring to efficiency, peak luminous intensity and spotlight dimension. The color uniformity level can be influenced by the light engine or the secondary optics but the mixing ability of the light engine has limitations. In conclusion, there is no optical system that provides optimal performance in each category.

A mixed light engine and plain reflector provide the best color mixing levels with regard to efficiency. A standard TIR lens is the best choice regarding peak luminous intensity. The shell mixer yields perfect color uniformity independent of the type of light source but at the cost of lower peak luminous intensity. The findings show that a specific combination of light engine and secondary optics is required depending on the application.

Acknowledgments

The authors would like to thank Alexandra Cvetkovic (LPI, Madrid, Spain) for providing us the shell mixer models. Furthermore, we thank Dennis Sprenger for creating the light engines and Andreas Dobner for his technical assistance (Osram GmbH, Regensburg, Germany).